Ibrutinib therapy releases leukemic surface IgM from antigen drive in chronic lymphocytic leukemia patients.

Samantha Drennan*,[1] Giorgia Chiodin*,[1] Annalisa D'Avola,[1] Ian Tracy,[1] Peter W. Johnson,[1] Livio Trentin,[2] Andrew J. Steele,[1] Graham Packham,[1] Freda K. Stevenson,[1] and Francesco Forconi.[1,3]

[1]Cancer Sciences Unit, Cancer Research UK and NIHR Experimental Cancer Medicine Centres, University of Southampton, Southampton, UK. [2]Padua University School of Medicine, Department of Medicine, Hematology and Clinical Immunology Branch, Padua, Italy. [3]Haematology Department, Cancer Care Directorate, University Hospital Southampton NHS Trust, Southampton, UK.

*These authors contributed equally to this work

Running Title: surface IgM recovery during ibrutinib therapy in CLL patients

Keywords: BTK, ibrutinib, B-cell receptor, chronic lymphocytic leukemia, antigen

This study was supported by Cancer Research UK (CRUK centre grant C34999/A18087), the Southampton Cancer Research UK and NIHR Experimental Cancer Medicine Centres at the University of Southampton, Bloodwise (grants 16003, 14037 and 12021), the Keanu Eyles Haematology Fellowship for the Cancer Immunology Centre, the Hairy Cell leukemia Foundation, and the Gilead UK & Ireland Oncology Fellowship Programme 2016.

Corresponding Author: Dr Francesco Forconi (ORCID reference: 0000-0002-2211-1831), MD, DM, PhD, FRCPath, Cancer Sciences Unit, University of Southampton, Cancer Research UK Centre, Somers Cancer Research Building, MP824, Southampton General Hospital, Southampton, SO16 6YD, UK. Email: f.forconi@soton.ac.uk. Tel: +44 (0)23 81205780 Fax: +44 (0)23 81205152

Conflict of interest disclosure: The authors declare no competing financial interests.

Abstract: 246 words.

Text: 4037 words.

Figures: 6

References: 50 references

Supplemental material: 2 tables and 5 figures

Translational relevance

In patients with chronic lymphocytic leukemia, the variable surface IgM levels inform signaling capacity, cell behavior and clinical progression. The drive on IgM signaling has been suspected to be antigen, mainly because surface IgM appears to undergo endocytosis *in vivo* and recovery *in vitro*. Daily ibrutinib therapy inhibits Bruton's tyrosine kinase (BTK)-dependent signaling and redistributes leukemic cells from tissue to blood. This study documents that the circulating CLL cells during therapy specifically increase surface IgM levels, retaining signaling function upstream of BTK. This observation provides, for the first time, evidence directly in patients that a key influence on the critical surface IgM of tumor cells is tissue antigen. This "experiment *in vivo*" tells us how leukemic cells behave and provides novel insight into surviving cells, which recover and retain potentially functional surface IgM during therapy.

ABSTRACT

Purpose: In chronic lymphocytic leukemia (CLL), disease progression associates with surface IgM (sIgM) levels and signaling capacity. These are variably down-modulated *in vivo* and recover *in vitro,* suggesting a reversible influence of tissue-located antigen. Therapeutic targeting of sIgM function via ibrutinib, an inhibitor of Bruton's tyrosine kinase (BTK), causes inhibition and tumor cell redistribution into the blood, with significant clinical benefit. Circulating CLL cells persist in an inhibited state, offering a tool to investigate the effects of drug on BTK-inhibited sIgM.

Experimental design: We investigated the consequences of ibrutinib therapy on levels and function of sIgM in circulating leukemic cells of CLL patients.

Results: At week 1, there was a significant increase of sIgM expression (64% increase from pre-therapy) on CLL cells either recently released from tissue or persisting in blood. In contrast, sIgD and a range of other receptors, did not change. SIgM levels remained higher than pre-therapy in the following 3 months, despite gradual cell size reduction and ongoing autophagy and apoptotic activity. Conversely, IgD and other receptors did not increase and gradually declined. Recovered sIgM was fully N-glycosylated, another feature of escape from antigen, and expression did not increase further during culture *in vitro*. The sIgM was fully capable of mediating phosphorylation of SYK which lies upstream of BTK in the B-Cell Receptor pathway.

Conclusions: This specific IgM increase in patients underpins the key role of tissue-based engagement with antigen in CLL, confirms the inhibitory action of ibrutinib, and reveals dynamic adaptability of CLL cells to precision monotherapy.

INTRODUCTION

B-cell receptor (BCR)-associated Bruton's tyrosine kinase (BTK) inhibitor ibrutinib has become a milestone for therapeutic success in chronic lymphocytic leukemia (CLL) and has been rapidly shifting patient treatment algorithms away from chemotherapy based regimens (1, 2). Inhibition of BTK by ibrutinib affects BCR signaling but also cell adhesion and migration (3-5), and induces a rapid and prominent lymph node reduction and redistribution of CLL cells into the peripheral blood (2, 6, 7). The prolonged CLL cell redistribution into the peripheral blood offers a unique way to interpret consequences of continuous separation of CLL surface receptors from their ligands in the tissue environment of patients, without need of models *in vitro* or in animals.

The BCR is the essential functional unit for most normal and neoplastic B-cells (8, 9). In CLL, BCR signaling is key to survival and proliferation, by affecting a multitude of cell functional components from signal transduction to translation and cell growth (8, 10, 11).

Analysis of the tumor BCR immunoglobulin (Ig) indicates that CLL consists of two major subsets with different origin and clinical behavior. The subset with unmutated (U) Ig gene heavy-chain variable regions (*IGHV*) has arisen from pre-germinal center $CD5^+$ B-cells and has a more aggressive clinical behavior, while the subset with mutated (M) *IGHV* has arisen from post-follicular $CD5^+$ B cells and generally is more indolent (12-16).

The circulating CLL cells from both subsets are characterized by low but variable surface IgM (sIgM) levels and signaling capacity (17). Although sIgM levels and signaling capacity are typically higher in U-CLL than in M-CLL (17-19), variability is evident in both subsets (17). This appears clinically important because cases with relatively higher sIgM levels/signaling capacity have a more rapid progression than those with lower sIgM levels/signaling capacity, (17) likely due to a larger proliferative component at tissue sites (20, 21).

Down-modulation of sIgM, but not of sIgD, levels and signaling capacity is a defining feature of antigen engagement (22). Chronic antigen engagement leads to anergy and is associated with increased basal phosphorylation levels of BCR signal-associated kinases, including spleen tyrosine kinase (SYK) and extracellular signal-regulated protein kinases 1/2 (ERK1/2)(22). This has been documented in transgenic mouse models (23, 24), and similar phenotypic and functional features have been described in human autoreactive B cells (25, 26). We and others have hypothesized that part of the variably reduced sIgM levels and signaling capacity in the circulating CLL cells is a consequence of chronic exposure to putative antigens (8). In support of this hypothesis we have documented that down-modulation of sIgM, but not of sIgD, is reversible in CLL cells when they are incubated in antigen-free media *in vitro* and that the recovery of sIgM levels associates with increased IgM-induced phosphorylation of SYK (18, 19). However, antigen-independent "autonomous" signaling by CLL BCRs has also been described *in vitro* (27). Although its relevance *in vivo,* where soluble Ig can compete, is unclear, this has opened the question if chronic BCR stimulation relies on tissue stimuli.

In this study, we examined the dynamics of sIgM levels and signaling capacity upstream to BTK of the tumor cells during their circulation in the blood stream of patients for the first 3 months of ibrutinib therapy. We document recovery of sIgM, but not of sIgD, which is the first *in vivo* evidence of direct antigen engagement specifically at tissue sites in CLL.

MATERIALS AND METHODS

Patients, ibrutinib treatment and cell preparation

Peripheral blood mononuclear cells (PBMCs) were collected from 13 patients with CLL requiring treatment (12 previously treated, and 1 previously untreated) prior to (pre-), and at week 1, month 1 and month 3 following the initiation of single-agent ibrutinib therapy. None of the patients had received any (immuno)chemotherapy or steroids for the 6 months prior to ibrutinib commencement. Following pre-ibrutinib sample collection, all patients received 420 mg ibrutinib once daily each morning and blood collection was performed no later than 2 hours from the daily ibrutinib administration. The study was approved by the Institutional Review Boards at the University of Southampton (REC: H228/02/t). All patients provided written informed consent.

Viable PBMCs were isolated by density gradient centrifugation and cryopreserved in fetal bovine serum (FBS) with 10% dimethyl sulfoxide (DMSO). Prior to each assay, PBMCs were thawed, washed, and allowed to recover for 1 hour at 37°C in complete RPMI1640 medium (supplemented with 10% FBS, 2mM glutamine and 1% penicillin/streptomycin). Tumor *IGHV* usage and mutational status, surface IgM and IgD levels and signaling capacity as measured by intracellular calcium mobilization assay, phenotypic CD38, CD49d, CXCR4 and ZAP70 expression and FISH characteristics according to Döhner classification at baseline were determined as described previously (7, 18, 28, 29).

Phenotypic analyses of CLL cells

PBMCs ($5x10^6$ cells/ml) were washed, re-suspended in FACS buffer (1% bovine serum albumin (BSA), 4mM EDTA, and 0.15 mM NaN_3 in phosphate buffered saline (PBS)) and stained for markers ($5x10^5$ cells/100µl) on ice for 30 minutes protected from light. The following antibody panels and corresponding isotype controls were used: PerCP/Cy5.5-conjugated anti-CD5 (UCHT2), Pacific Blue-conjugated anti-CD19 (HIB19) or APC/Cy7-conjugated anti-CD19 (HIB19), PE-conjugated anti-IgM (MHM-88), APC-conjugated anti-CXCR4 (12G5) or anti-CD32b (FcγRIIb. 6G11) (kind gift from Prof. Mark Cragg, CSU, Southampton) and FITC conjugated anti-IgD (IA6-2), or anti-CD38 (HB-7), or anti-CD49d (9F10), or anti-CD20 (2H7) (all from Biolegend, London, UK). Following incubation, cells were washed, re-suspended in FACS buffer and $1x10^4$ lymphocytes were acquired on a FACS Canto (BD Biosciences, Oxford, UK). Expression was determined as geometric mean fluorescence intensity (MFI) of test sample subtracted by the relevant isotype control MFI on $CD19^+CD5^+$ CLL cells, using FlowJo software (FlowJo, LLC, Ashland, OR, USA). In order to compare results at different time points, when CLL cell size was different (**Supplementary Figure S1**), density of surface markers was measured as the ratio between MFI and forward scatter squared (FSC^2) (30).

BCR stimulation and immunoblotting

Recovered PBMCs ($1x10^7$/ml) were stimulated with polyclonal goat $F(ab')_2$ anti-human IgM, soluble polyclonal control (20µg/ml; Southern Biotech, Cambridge, UK) or left unstimulated at 37°C for 10 minutes. For immunoblotting, cells were washed twice in ice-cold PBS and incubated for 30 minutes on ice in RIPA buffer (150mM NaCl, 1% NP-40, 0.5% sodium deoxycholate, 0.1% sodium-dodecyl-sulphate (SDS), 50 mM tris(hydroxymethyl)aminomethane hydrochloride (Tris-HCL), pH 8.0), containing 1X protease inhibitor and phosphatase inhibitor cocktail 2 and 3 (Sigma-Aldrich, Gillingham, UK). Protein concentration was determined using the Pierce BCA Protein Assay Kit (Thermo Fisher Scientific, Loughborough, UK). Equivalent protein amounts were boiled for 5 minutes in Red Loading buffer and dithiothreitol (DTT; Cell Signaling Technology, Hitchin, UK), separated by SDS 10% polyacrylamide gel electrophoresis (SDS-PAGE) and transferred to nitrocellulose membranes (GE Healthcare, Amersham, UK). After blocking with 5% BSA in Tris-buffered saline, the membranes were probed with the required primary antibody and subsequently stained with horseradish peroxidase-conjugated secondary antibodies (Dako, Agilent

Technologies, Stockport, UK). Following enhancement by chemiluminescence reagents (Pierce ECL and SuperSignal West Femto, Thermo Fisher Scientific), proteins were visualized using the ChemiDoc-It imaging system (UVP, Cambridge, UK). Primary antibodies used were anti-phosphoBTK (Tyr223), anti-BTK (D3H5), anti-phosphoSYK (Tyr525/526) (C87C1), anti-SYK, anti-LC3B (D11), anti-Bim, anti-Bcl-xL (54H6) (Cell Signaling Technology), anti-Mcl-1 (Santa Cruz Biotechnology, Heidelberg, Germany), anti-Bcl-2 (124) (Dako), anti-β-actin (AC-15) (Sigma) and anti-GAPDH (6C5) (Ambion, Loughborough, UK). Band optical density (OD) was quantified using ImageJ and normalized to the loading control β-actin or GAPDH, the levels of phospho-proteins were further normalized on the levels of the respective total proteins. 'Basal' and 'induced' phosphoprotein levels were defined as [test phosphoprotein OD/test total protein OD] in the absence and in the presence of stimulation by anti-IgM *in vitro*, respectively. 'Inducibility' was defined as the ratio of induced/basal phosphoprotein levels at each time point.

Biotinylation and glycosylation analysis of cell surface IgM

Cell surface proteins were biotinylated and isolated using the Cell Surface Protein Isolation kit (Pierce, Thermo Fisher Scientific), as previously described (31). Cell surface glycosylation patterns were determined by digestion with endoglycosidase H (EndoH; New England Biolabs, Hitchin, UK) which removes only the mannosylated N-glycans characteristic of the immature IgM form, but does not affect the mature IgM form, or peptide:N-glycosidase F (PNGase; New England Biolabs), which removes all attached N-glycans (31). Biotinylated proteins were analyzed by immunoblotting using the primary antibody anti-μ (Jackson ImmunoResearch Laboratories, Stratech Scientific, Newmarket, UK).

Statistics

Continuous variables were compared by Wilcoxon-signed rank non-parametric test. For statistical correlation between two variables, the non-parametric Spearman's rank test was used. All statistical tests were 2-sided. Statistical significance was defined as *P*-value <0.05. Analyses were performed with GraphPad Prism 6 software (La Jolla, CA, USA).

RESULTS

Complete inhibition of BTK phosphorylation capacity following anti-IgM stimulation during ibrutinib therapy

Twelve CLL patients were investigated for phenotypic and functional changes prior to (pre-), and at week 1, at month 1 and at month 3 following the initiation of single-agent ibrutinib therapy (**Supplementary Table S1**). Prior to ibrutinib commencement, mean sIgM levels and signaling capacity were relatively high and similar to those in patients with progressive CLL in 11/12 patients investigated (mean fluorescence intensity (MFI) mean 102, range 24-221 and IgM iCa^{2+} % mean 40, range 16-77) (17). The one case (489) that had low levels/signaling capacity was an exception. Time points chosen for analysis post-treatment initiation were week 1, when blood lymphocyte counts were increasing in all patients (fold increase range from pre-therapy 1.4-3.5, mean 2.1), month 1 and month 3 (**Supplementary Table S2**). Basal BTK phosphorylation was decreased at all time points during ibrutinib therapy from week 1 to month 3 compared to pre-therapy (**Supplementary Figure S2A-C**). Following stimulation with anti-IgM, BTK phosphorylation levels increased significantly prior to ibrutinib commencement, whereas no response was detectable during therapy in all patients (**Supplementary Figure S2A-C**). The reduced basal BTK phosphorylation and the

inhibition of anti-IgM-induced BTK phosphorylation capacity at week 1 and at subsequent time points confirmed that ibrutinib was operating *in vivo* at the time of blood collection.

Specific early increase of surface IgM expression, but not of other surface markers, on CLL cells during ibrutinib therapy

Expression of molecules involved in BCR signaling (IgM, IgD, CD19, CD32b) or adhesion (CD38, CD49d) and of CD20 was determined on the circulating CLL cells before and during ibrutinib therapy.

At week 1, a significant increase of sIgM expression was observed on the tumor cells of 11/12 cases (**Figure 1A**). The only exception was case 489, which had very low sIgM levels and signaling capacity since before treatment commencement and failed to increase sIgM expression. The increase occurred in both U-CLL and M-CLL (**Figure 1A**). A representative case is shown in **Figure 1B**. The mean MFI of the 11/12 responders was 64% higher at week 1 than pre-therapy. In contrast, expression of other markers, including sIgD, did not change or slightly decreased, while down-modulation of CD20 was already particularly evident at this early time-point (**Figure 1A-B**).

In order to compare the changes of surface molecule expression at different time points, when CLL cell size was different, we normalized expression by dividing receptor MFI with FSC^2 at each time point. In fact, by using forward scatter (FSC) as an indicator of cell size (32-34), we observed that CLL cells significantly and gradually reduced in size at months 1 and 3 of therapy in all cases ($P \leq 0.001$; **Supplementary Figure S1A**). Reduction of CLL cell size was accompanied by a significant increase of LC3BII ($P=0.02$) at month 3 of therapy, to indicate autophagosome formation (35) (**Supplementary Figure S1B**). At this time point, there was also specific increase of pro-apoptotic Bim-EL levels ($P=0.02$), while Mcl-1, Bcl-xL and Bcl-2 levels remained stable in the circulating CLL cells *in vivo* (**Supplementary Figure S1C**). This suggested promotion of specific Bim-mediated apoptosis events (36, 37).

Despite reduction of cell size, sIgM density at months 1 and 3 remained higher than baseline values observed prior to therapy (**Figure 2** and **Supplementary Figure S3**). In marked contrast, all the other receptors examined significantly reduced expression at these later time points ($P<0.01$; **Figure 2** and **Supplementary Figure S3**). This reflected a real reduction in surface density in the size-contracted cells. The reduction included sIgD, and appeared particularly pronounced for CD20.

The specific early dissociation of trends between sIgM levels, which increased during therapy, and sIgD levels, which reduced in a fashion similar to the other receptors measured, was highly suggestive of a distinct influence operating specifically on the sIgM, potentially involving antigen disengagement (22, 25, 26).

We focused our analyses on sIgM at week 1. The later time points were not investigated further because of the significant changes of cell size with ongoing autophagy/apoptosis (**Supplementary Figure S1**), which makes biological interpretation of sIgM changes more complex.

The increase of surface IgM expression occurs in both the recently egressed and the persistently circulating CLL cell populations

It has been reported that CLL cells recently egressed from tissue sites have diminished expression of CXCR4 and relatively high expression of CD5 ($CXCR4^{dim}CD5^{hi}$), while those that have been persisting in the circulation are $CXCR4^{bright}CD5^{low}$ (38). We determined sIgM expression in both fractions at pre-therapy and week 1. Both the $CXCR4^{dim}CD5^{hi}$ and the

$CXCR4^{bright}CD5^{low}$ absolute cell counts increased in the peripheral blood. On average, the relative proportion of the recently egressed fraction was higher (mean percentage 33% of the total CLL population pre-therapy, 39% at week 1) while the $CXCR4^{bright}CD5^{low}$ fraction was lower (mean percentage, 28% pre-therapy, 23% at week 1; **Figure 3A-B**), although the differences were not significant. SIgM expression was higher in the recently egressed cells than in the persistently circulating cells. However, sIgM increase was significant and similar in both the $CXCR4^{dim}CD5^{hi}$ cells and the $CXCR4^{bright}CD5^{low}$ cells (**Figure 3C**, ~40% increase from pre-therapy in both fractions, and **Supplementary Figure S4**). These data indicated that sIgM increased in all fractions during ibrutinib therapy. They suggested that the increase was not simply a reflection of the redistribution of subpopulations with different sIgM levels (39).

The raised expression of surface IgM on the blood CLL cells during ibrutinib therapy does not increase further during incubation in vitro

We have previously shown that sIgM, but not sIgD, expression and signaling capacity recover spontaneously *in vitro* (18). Those observations were obtained from peripheral blood CLL cells that had not been inhibited by ibrutinib and hence that had been exposed to tissue interactions (40, 41). Here we determined sIgM expression changes *in vitro* in 4 CLL samples (409, 531, 551, 601) prior to or at week 1 of ibrutinib therapy (**Figure 4**)**.** From analysis of the samples obtained pre-therapy, sIgM (but not sIgD) levels on the CLL cells increased following culture *in vitro* for 48 hours in all 4 patients (531, 35%; 551, 42%; 409, 103%; and 601, 194% increase, **Figure 4B-C**), as expected (18). The increase in sIgM expression occurred both when ibrutinib was added and when ibrutinib was not added *in vitro* (**Figure 4B**). The sIgM increases after 48 hours culture of the pre-therapy samples ***in vitro*** were similar to (cases 409, 531 and 601) or lower (case 551) than those observed at week 1 of therapy from the same patient. From analysis of the samples obtained at week 1 of ibrutinib therapy, no further significant increase in sIgM expression could be achieved following culture *in vitro* for 48 hours (**Figure 4B**). To investigate a potentially direct effect of ibrutinib on expression of sIgM, we exposed a B-cell line to ibrutinib at different concentrations *in vitro*. The results document that ibrutinib per se does not lead to an increase in sIgM expression, but may actually reduce expression, especially at the higher concentration where toxicity is more likely (**Supplementary Figure S5**). This indicated that ibrutinib therapy had allowed recovery of sIgM expression. Since the increase was occurring *in vivo,* on cells persisting in the blood circulation, and the drug had no direct increasing effect *in vitro*, we reasoned that the specific sIgM increase was due to prolonged disengagement from tissue antigen.

Increased surface IgM expression is associated with mature fully N-glycosylated µ-chains

We have shown previously that the N-glycosylation status of the glycans in the IgM heavy chain constant region varies in CLL cells from the blood (31). This reflects the level of activation of the cell, with immature glycan predominating in the blood, but mature glycan returning with recovery of sIgM expression *in vitro*. An increasing ratio of mature/immature IgM glycoform is therefore an index of antigen-free recovery (31).

We assessed the N-glycosylation status of the sIgM µ-chains in samples from 3 patients, 2 of which had increased sIgM levels on ibrutinib (551 and 343) and the single outlier which had maintained similarly very low sIgM levels pre- and on ibrutinib therapy (489; **Figure 5**). The ratio of mature to immature glycoforms increased in both the patients with increased sIgM, while it did not change in the patient that did not increase sIgM levels. In fact, the sample that had the greatest increase in sIgM expression (551) also had the greatest increase in the expression of the mature glycoform. These data are consistent with the established recovery of the mature fully N-glycosylated form of sIgM during incubation *in*

vitro (31), and support the hypothesis that ibrutinib therapy is mimicking this situation by preventing access of the cells to putative antigen *in vivo* (18, 31). Case 489 presents an interesting exception where, still in the absence of the most common recurrent genomic changes (**Supplementary Table S1**), there appears to be a profile of chronic and severe anergy, which is not recoverable either by blocking BTK *in vivo* or by incubation *in vitro*.

Surface IgM recovery is accompanied by loss of chronic antigen stimulation signature but retention of inducible SYK phosphorylation

Constitutive activation of SYK and of downstream kinases is a hallmark of chronic stimulation by antigen (42). We examined our 12 cases for changes in the activation status of SYK following ibrutinib commencement. We found that basal phosphorylation of SYK during ibrutinib therapy was significantly lower than prior to treatment in all the 12 cases investigated. Three representative cases are shown in **Figure 6A** (P=0.001). This indicated loss of stimulation by antigen when the tumor cells are exiled in the blood circulation by continuous ibrutinib therapy.

The induced phosphorylation of SYK, which is upstream of BTK, was measured to determine if the elevated levels of sIgM on the CLL cells were functional during ibrutinib. The ability of anti-IgM to induce SYK phosphorylation was measured as the ratio of sIgM-mediated pSYK (OD): basal pSYK (OD) levels (pSYK inducibility). SIgM mediated inducibility of SYK at week 1 was greater than pre-therapy (P=0.01, **Figure 6B-C**). Inducibility correlated both with overall sIgM levels at week 1 (r=0.64, P=0.03, **Figure 6D**) and with the differential increase of sIgM levels (**Figure 6E**). However, the greater inducibility was a reflection of the fall in basal levels of phosphorylated SYK during ibrutinib therapy, while maximal total phosphorylation capacity was overall similar pre-therapy and during ibrutinib. These results demonstrate maintained capacity of anti-IgM to induce SYK whilst on ibrutinib therapy and indicate that the increased sIgM observed is functional.

DISCUSSION

The sIgM is a known influence on CLL behavior, and its level or signaling capacity correlates with disease progression (17). Clinical responses to drugs such as the BTK inhibitor ibrutinib, which acts on BCR-associated pathways, are consistent with this. However the effects of ibrutinib are not exclusive to this pathway, with known inhibition of chemokine-mediated migration and of adhesion, features important in mediating redistribution of CLL cells in the peripheral blood (3-5).

We have investigated the status of sIgM on circulating CLL cells of patients during the initial months of ibrutinib therapy, when lymphocytosis was present. We observed a significant increase in sIgM expression in the first week of therapy. The expression remained higher than pre-therapy levels at subsequent time points, despite a significant decrease in CLL cell size. This contrasted with the reduction of expression of all the other surface receptors investigated, including sIgD. While the parallel decreases in several cell surface markers may simply reflect a contracting cell size with the ongoing autophagocytic events, downregulation of CD20 appeared more significant and has been explained to be caused by the prevention of access of tumor lymphocytes to chemokine-producing stromal cells in tissue sites by ibrutinib therapy (43).

The distinctive behavior of sIgM as compared with sIgD is highly suggestive of a specific role for antigen disengagement which then allows sIgM recovery (23, 24). This discriminatory effect on sIgM is seen in normal human B cells anergized by chronic antigen exposure (25,

26). The degree of recovery of expression and the presence of the mature glycoform of sIgM in CLL cells from ibrutinib-treated patients point to a complete re-expression of sIgM to levels similar to that obtained by culturing pre-therapy cells under exogenous 'antigen-free' conditions (18). Our findings now add a new direct tier of evidence that antigen engagement occurs at specific tissue sites.

By using ibrutinib as a 'tool' *in vivo* to inhibit redistribution in tissue sites (e.g. lymph node or bone marrow) our analysis revealed that the CLL cells within the patients had the capacity to fully recover and maintain expression of sIgM. Recent studies *in vitro* have raised the hypothesis that BCR levels and signaling are regulated by antigen-independent mechanisms, including 'autonomous' signaling or distinct homotypic B-cell receptor interactions (27, 44). Either hypotheses imply heterogeneous, but tumor specific structure characteristics intrinsic and unique to the CLL cell BCRs. However we found that the Ig structures appear no dissimilar from those of the normal B-cell repertoire (13), and soluble Ig in the blood can compete *in vivo*. Also the specific level and signaling recovery that affect IgM, but not IgD, in CLL circulating cells would be difficult to explain with autonomous signaling, which would operate in all tumor compartments. Instead, the modulation could be explained by the evidence *in vivo* (mouse models) provided by the same investigators of selection and expansion of the CLL clone by pathogen-specific BCRs that cross-react with one or more self-antigens (45). Our current study highlights for the first time in patients that CLL IgM modulation and maturation is regulated by tissue-based antigens.

Ibrutinib is known to prevent the return of circulating CLL cells to tissue sites, while egress will continue (46). The circulating cells at week 1 will therefore include two fractions, identified as the $CXCR4^{dim}CD5^{hi}$ recently egressed fraction, possibly with higher levels of CD20 (43), and the $CXCR4^{bright}CD5^{low}$ persisting fraction, respectively (38). The proportions are difficult to estimate and the phenotype is likely to change over time *in vitro* and *in vivo* (39, 43). When the recently egressed and the persistently circulating fractions were identified by means of these markers, we observed that sIgM was higher in the recently egressed CLL cells. Interactions of CLL cells with tissue environmental cells will affect levels of functional BCR IgM/D complex (47). We and others have speculated that the higher sIgM might be a consequence of expression enhancement by tissue-derived interleukin-4 (48, 49). However, both fractions increased their relative sIgM levels during therapy, suggesting that the reversible downregulation of sIgM due to antigen is a feature of both recent tissue emigrants and of those circulating in the peripheral blood, where the imprint of antigen engagement is still partially evident (18).

In terms of functional capacity of the recovered sIgM, there is a clear blockade of BTK activity in drug-treated patients but the ability of anti-IgM to phosphorylate SYK, which lies upstream of BTK, is still present. Basal levels of pSYK can be detected in CLL cells at the pre-treatment stage, which can be explained by antigen engagement *in vivo* (18). These levels decline on ibrutinib treatment, again pointing to a block on access to tissue-based stimuli (50).

The data on sIgM expression therefore reveal that the effect of ibrutinib on CLL cells *in vivo* is best explained by the prevention of access of circulating cells to tissue sites, probably by inhibiting chemokine-mediated migration (3-5). The lack of a nourishing signal from (auto)antigen then consigns the CLL cells to a circulating *limbo* where they survive for some time, possibly due to maintained anti-apoptotic strategies, but slowly contract in size. The recovery of sIgM in the absence of antigen engagement argues that tissue-localized antigen is the likely driver of proliferation. One question is whether the CLL cells *in limbo,* which are presumably prevented from tissue access by ibrutinib, but which retain proximal signaling function, should be removed by a second level of therapeutic attack.

ACKNOWLEDGMENTS

We would like to thank Mrs Isla Henderson (supported by the ECMC C24563/A15581 grant), Dr Kathy Potter and Ms Carina Mundy (supported by the Hairy Cell Leukemia Foundation) for sample identification, collection and storage in the South Coast Tissue Bank (Bloodwise grant 16003).

REFERENCES

1. Burger JA. Inhibiting B-cell receptor signaling pathways in chronic lymphocytic leukemia. Current hematologic malignancy reports. 2012;7(1):26-33.
2. Byrd JC, Furman RR, Coutre SE, Flinn IW, Burger JA, Blum KA, et al. Targeting BTK with ibrutinib in relapsed chronic lymphocytic leukemia. N Engl J Med. 2013;369(1):32-42.
3. Chen SS, Chang BY, Chang S, Tong T, Ham S, Sherry B, et al. BTK inhibition results in impaired CXCR4 chemokine receptor surface expression, signaling and function in chronic lymphocytic leukemia. Leukemia. 2016;30(4):833-43.
4. de Rooij MF, Kuil A, Geest CR, Eldering E, Chang BY, Buggy JJ, et al. The clinically active BTK inhibitor PCI-32765 targets B-cell receptor- and chemokine-controlled adhesion and migration in chronic lymphocytic leukemia. Blood. 2012;119(11):2590-4.
5. Herman SE, Mustafa RZ, Jones J, Wong DH, Farooqui M, Wiestner A. Treatment with Ibrutinib Inhibits BTK- and VLA-4-Dependent Adhesion of Chronic Lymphocytic Leukemia Cells In Vivo. Clin Cancer Res. 2015;21(20):4642-51.
6. Wodarz D, Garg N, Komarova NL, Benjamini O, Keating MJ, Wierda WG, et al. Kinetics of CLL cells in tissues and blood during therapy with the BTK inhibitor ibrutinib. Blood. 2014;123(26):4132-5.
7. Tissino E, Benedetti D, Herman SEM, Ten Hacken E, Ahn IE, Chaffee KG, et al. Functional and clinical relevance of VLA-4 (CD49d/CD29) in ibrutinib-treated chronic lymphocytic leukemia. J Exp Med. 2018.
8. Stevenson FK, Forconi F, Packham G. The meaning and relevance of B-cell receptor structure and function in chronic lymphocytic leukemia. Seminars in hematology. 2014;51(3):158-67.
9. Lam KP, Kuhn R, Rajewsky K. In vivo ablation of surface immunoglobulin on mature B cells by inducible gene targeting results in rapid cell death. Cell. 1997;90(6):1073-83.
10. Packham G, Krysov S, Allen A, Savelyeva N, Steele AJ, Forconi F, et al. The outcome of B-cell receptor signaling in CLL: proliferation or anergy? Haematologica. 2014;99(9):1-11.
11. Yeomans A, Thirdborough SM, Valle-Argos B, Linley A, Krysov S, Hidalgo MS, et al. Engagement of the B-cell receptor of chronic lymphocytic leukemia cells drives global and MYC-specific mRNA translation. Blood. 2016;127(4):449-57.
12. Seifert M, Sellmann L, Bloehdorn J, Wein F, Stilgenbauer S, Durig J, et al. Cellular origin and pathophysiology of chronic lymphocytic leukemia. J Exp Med. 2012;209(12):2183-98.
13. Forconi F, Potter KN, Wheatley I, Darzentas N, Sozzi E, Stamatopoulos K, et al. The normal IGHV1-69-derived B-cell repertoire contains stereotypic patterns characteristic of unmutated CLL. Blood. 2010;115(1):71-7.
14. Stevenson FK, Sahota SS, Ottensmeier CH, Zhu D, Forconi F, Hamblin TJ. The occurrence and significance of V gene mutations in B cell-derived human malignancy. Adv Cancer Res. 2001;83:81-116.
15. Damle RN, Wasil T, Fais F, Ghiotto F, Valetto A, Allen SL, et al. Ig V gene mutation status and CD38 expression as novel prognostic indicators in chronic lymphocytic leukemia. Blood. 1999;94(6):1840-7.
16. Hamblin TJ, Davis Z, Gardiner A, Oscier DG, Stevenson FK. Unmutated Ig V(H) genes are associated with a more aggressive form of chronic lymphocytic leukemia. Blood. 1999;94(6):1848-54.
17. D'Avola A, Drennan S, Tracy I, Henderson I, Chiecchio L, Larrayoz M, et al. Surface IgM expression and function are associated with clinical behavior, genetic abnormalities, and DNA methylation in CLL. Blood. 2016;128(6):816-26.
18. Mockridge CI, Potter KN, Wheatley I, Neville LA, Packham G, Stevenson FK. Reversible anergy of sIgM-mediated signaling in the two subsets of CLL defined by VH-gene mutational status. Blood. 2007;109(10):4424-31.

19. Lanham S, Hamblin T, Oscier D, Ibbotson R, Stevenson F, Packham G. Differential signaling via surface IgM is associated with VH gene mutational status and CD38 expression in chronic lymphocytic leukemia. Blood. 2003;101(3):1087-93.
20. Krysov S, Dias S, Paterson A, Mockridge CI, Potter KN, Smith KA, et al. Surface IgM stimulation induces MEK1/2-dependent MYC expression in chronic lymphocytic leukemia cells. Blood. 2012;119(1):170-9.
21. Zhang W, Kater AP, Widhopf GF, 2nd, Chuang HY, Enzler T, James DF, et al. B-cell activating factor and v-Myc myelocytomatosis viral oncogene homolog (c-Myc) influence progression of chronic lymphocytic leukemia. Proc Natl Acad Sci U S A. 2010;107(44):18956-60.
22. Yarkoni Y, Getahun A, Cambier JC. Molecular underpinning of B-cell anergy. Immunol Rev. 2010;237(1):249-63.
23. Merrell KT, Benschop RJ, Gauld SB, Aviszus K, Decote-Ricardo D, Wysocki LJ, et al. Identification of anergic B cells within a wild-type repertoire. Immunity. 2006;25(6):953-62.
24. Goodnow CC, Crosbie J, Adelstein S, Lavoie TB, Smith-Gill SJ, Brink RA, et al. Altered immunoglobulin expression and functional silencing of self-reactive B lymphocytes in transgenic mice. Nature. 1988;334(6184):676-82.
25. Duty JA, Szodoray P, Zheng NY, Koelsch KA, Zhang Q, Swiatkowski M, et al. Functional anergy in a subpopulation of naive B cells from healthy humans that express autoreactive immunoglobulin receptors. J Exp Med. 2009;206(1):139-51.
26. Quach TD, Manjarrez-Orduno N, Adlowitz DG, Silver L, Yang H, Wei C, et al. Anergic responses characterize a large fraction of human autoreactive naive B cells expressing low levels of surface IgM. J Immunol. 2011;186(8):4640-8.
27. Duhren-von Minden M, Ubelhart R, Schneider D, Wossning T, Bach MP, Buchner M, et al. Chronic lymphocytic leukaemia is driven by antigen-independent cell-autonomous signalling. Nature. 2012;489(7415):309-12.
28. Dohner H, Stilgenbauer S, Benner A, Leupolt E, Krober A, Bullinger L, et al. Genomic aberrations and survival in chronic lymphocytic leukemia. N Engl J Med. 2000;343(26):1910-6.
29. Forconi F, Sahota SS, Raspadori D, Mockridge CI, Lauria F, Stevenson FK. Tumor cells of hairy cell leukemia express multiple clonally related immunoglobulin isotypes via RNA splicing. Blood. 2001;98(4):1174-81.
30. Michaels AD, Newhook TE, Adair SJ, Morioka S, Goudreau BJ, Nagdas S, et al. CD47 Blockade as an Adjuvant Immunotherapy for Resectable Pancreatic Cancer. Clin Cancer Res. 2017.
31. Krysov S, Potter KN, Mockridge CI, Coelho V, Wheatley I, Packham G, et al. Surface IgM of CLL cells displays unusual glycans indicative of engagement of antigen in vivo. Blood. 2010;115(21):4198-205.
32. O'Sullivan D, van der Windt GJ, Huang SC, Curtis JD, Chang CH, Buck MD, et al. Memory CD8(+) T cells use cell-intrinsic lipolysis to support the metabolic programming necessary for development. Immunity. 2014;41(1):75-88.
33. Xu X, Araki K, Li S, Han JH, Ye L, Tan WG, et al. Autophagy is essential for effector CD8(+) T cell survival and memory formation. Nat Immunol. 2014;15(12):1152-61.
34. Cotrell A, Sayedian F, Huang M, Chen X, Xie M, Smith M, et al. Flow Cytometric Analysis of Cell Size in B-Cell Non-Hodgkin Lymphoma: Reliability and Potential Diagnostic Significance. International Journal of Pathology and Clinical Research. 2015;1(1).
35. Codogno P, Mehrpour M, Proikas-Cezanne T. Canonical and non-canonical autophagy: variations on a common theme of self-eating? Nat Rev Mol Cell Biol. 2011;13(1):7-12.
36. Kuwana T, Bouchier-Hayes L, Chipuk JE, Bonzon C, Sullivan BA, Green DR, et al. BH3 domains of BH3-only proteins differentially regulate Bax-mediated mitochondrial membrane permeabilization both directly and indirectly. Mol Cell. 2005;17(4):525-35.
37. Bouillet P, Metcalf D, Huang DC, Tarlinton DM, Kay TW, Kontgen F, et al. Proapoptotic Bcl-2 relative Bim required for certain apoptotic responses, leukocyte homeostasis, and to preclude autoimmunity. Science. 1999;286(5445):1735-8.

38. Calissano C, Damle RN, Marsilio S, Yan XJ, Yancopoulos S, Hayes G, et al. Intraclonal complexity in chronic lymphocytic leukemia: fractions enriched in recently born/divided and older/quiescent cells. Mol Med. 2011;17(11-12):1374-82.
39. Coelho V, Krysov S, Steele A, Sanchez Hidalgo M, Johnson PW, Chana PS, et al. Identification in CLL of circulating intraclonal subgroups with varying B-cell receptor expression and function. Blood. 2013;122(15):2664-72.
40. Manaster J, Fruhling J, Stryckmans P. Kinetics of lymphocytes in chronic lymphocytic leukemia. I. Equilibrium between blood and a "readily accessible pool". Blood. 1973;41(3):425-38.
41. Gowans JL. The recirculation of lymphocytes from blood to lymph in the rat. J Physiol. 1959;146(1):54-69.
42. Apollonio B, Scielzo C, Bertilaccio MT, Ten Hacken E, Scarfo L, Ranghetti P, et al. Targeting B-cell anergy in chronic lymphocytic leukemia. Blood. 2013;121(19):3879-88, S1-8.
43. Pavlasova G, Borsky M, Seda V, Cerna K, Osickova J, Doubek M, et al. Ibrutinib inhibits CD20 upregulation on CLL B cells mediated by the CXCR4/SDF-1 axis. Blood. 2016;128(12):1609-13.
44. Minici C, Gounari M, Ubelhart R, Scarfo L, Duhren-von Minden M, Schneider D, et al. Distinct homotypic B-cell receptor interactions shape the outcome of chronic lymphocytic leukaemia. Nat Commun. 2017;8:15746.
45. Jimenez de Oya N, De Giovanni M, Fioravanti J, Ubelhart R, Di Lucia P, Fiocchi A, et al. Pathogen-specific B-cell receptors drive chronic lymphocytic leukemia by light-chain-dependent cross-reaction with autoantigens. EMBO Mol Med. 2017;9(11):1482-90.
46. Herman SE, Niemann CU, Farooqui M, Jones J, Mustafa RZ, Lipsky A, et al. Ibrutinib-induced lymphocytosis in patients with chronic lymphocytic leukemia: correlative analyses from a phase II study. Leukemia. 2014;28(11):2188-96.
47. Ten Hacken E, Sivina M, Kim E, O'Brien S, Wierda WG, Ferrajoli A, et al. Functional Differences between IgM and IgD Signaling in Chronic Lymphocytic Leukemia. J Immunol. 2016;197(6):2522-31.
48. Aguilar-Hernandez MM, Blunt MD, Dobson R, Yeomans A, Thirdborough S, Larrayoz M, et al. IL-4 enhances expression and function of surface IgM in CLL cells. Blood. 2016;127(24):3015-25.
49. Guo B, Zhang L, Chiorazzi N, Rothstein TL. IL-4 rescues surface IgM expression in chronic lymphocytic leukemia. Blood. 2016;128(4):553-62.
50. Gauld SB, Benschop RJ, Merrell KT, Cambier JC. Maintenance of B cell anergy requires constant antigen receptor occupancy and signaling. Nat Immunol. 2005;6(11):1160-7.

FIGURE LEGENDS

Figure 1. Surface IgM expression is elevated on CLL cells at week 1 of ibrutinib therapy. PBMCs were taken pre- and at week 1 of ibrutinib therapy and analyzed for cell surface marker expression (n=12). (**A**) Left panel shows surface IgM (sIgM) mean fluorescence intensity (MFI) following subtraction of isotype control MFI. Each symbol identifies one individual patient (refer to **Supplementary Table S1**). Open symbols represent U-CLL, closed symbols represent M-CLL. Horizontal lines indicate mean values. Right panel shows fold change for the expression of each marker compared with pre-therapy in the 12 patients. Pre-therapy values were normalized to one (dashed line). Horizontal lines indicate mean values. The statistical significance of difference was analyzed using the Wilcoxon-signed rank test of the MFI values prior to and during ibrutinib (week 1). P-values are represented for sIgM and CD20, where significant changes were observed; ***P ≤ 0.001. P-value was not significant for all other markers. (**B**) An example (case 644) of the flow cytometric plots. Grey line indicates expression at pre-therapy, black line indicates expression at week 1 of therapy, dashed grey line indicates isotype control.

Figure 2. Surface expression of receptors on CLL cells during the first three months of ibrutinib therapy. PBMCs were taken at pre-, week 1, month 1 or month 3 of ibrutinib therapy and analyzed for cell surface marker expression taking into account CLL cell size. For each marker the test MFI was divided by FSC^2. Pre-therapy values were normalized to one (white bar). Each bar represents mean with standard error of the mean. The statistical significance of difference was analyzed using the Wilcoxon-signed rank test of the FSC adjusted MFI values. *P < 0.05; **P < 0.01; ***P ≤ 0.001

Figure 3. Both $CXCR4^{dim}CD5^{hi}$ and $CXCR4^{bright}CD5^{low}$ fractions increase sIgM expression on ibrutinib therapy. PBMCs were taken pre- and at week 1 of ibrutinib therapy (n=12). The $CXCR4^{dim}CD5^{hi}$ and $CXCR4^{bright}CD5^{low}$ fractions were separated at the point where there was the highest density of events in the plot of the CLL population at pre- and the gates were maintained for comparisons at subsequent time points. (**A**) Representative plot (case 531) showing the gating strategy to identify the $CXCR4^{dim}CD5^{hi}$ and $CXCR4^{bright}CD5^{low}$ fractions. (**B**) The percentage of CLL cells expressing $CXCR4^{dim}CD5^{hi}$ and $CXCR4^{bright}CD5^{low}$ in all 12 CLL patients. The statistical significance of difference was analyzed using the Wilcoxon-signed rank test; NS = not significant. (**C**) The expression of sIgM by the $CXCR4^{dim}CD5^{hi}$ and $CXCR4^{bright}CD5^{low}$ fractions in all 12 CLL patients is shown as MFI (left panel) or fold change (right panel; pre-therapy values were normalized to one). Each symbol identifies one individual patient (refer to **Supplementary Table S1**). Open symbols represent U-CLL, closed symbols represent M-CLL. Horizontal lines indicate mean values. Filled bars identify mean fold changes with standard error of the means. The statistical significance of difference was analyzed using the Wilcoxon-signed rank test. *P < 0.05; **P < 0.01.

Figure 4. Expression of sIgM on the circulating CLL cells during ibrutinib therapy is not accompanied by further recovery *in vitro*. PBMCs were obtained pre- and at week 1 of ibrutinib therapy. (**A**) Left panel: an example (case 409) of the flow cytometric plots from the pre-therapy sample showing the expression of sIgM at baseline (black line) and following *in vitro* culture of PBMCs ($5x10^6$/ml) in a 96-well flat bottom plate for 48hrs (black dashed line) (18). Center panel: the expression of sIgM in the pre-therapy sample following 48 hours of *in vitro* culture (black dashed line) reached a level similar to that observed at week 1 of ibrutinib therapy *in vivo* (grey line). Right panel: the expression of sIgM at week 1 of ibrutinib therapy (grey line) did not increase any further following *in vitro* culture for 48hrs (grey dashed line). (**B**) Expression of sIgM and (**C**) sIgD in samples obtained by 4 patients (409, 531, 551, 601) pre-therapy (upper panel) or following 1 week of therapy (lower panel) measured at baseline (0 hours) and following *in vitro* culture for 48 hours. Baseline sIgM or

sIgD values pre-therapy (black bars) or at week 1 (grey bars) were normalized to one. Mean fold changes with standard error of the means in the absence (black dashed bars for pre-therapy, grey dashed bars for week 1) or in the presence of 10µM ibrutinib *in vitro* (white bars with black border for pre-therapy, white bars with grey border for week 1), respectively, were calculated. The statistical significance of difference was analyzed using the Mann-Whitney test. *: P<0.05. ns: not significant.

Figure 5. SIgM expression on the circulating CLL cells during ibrutinib therapy is associated with fully N-glycosylated form of the µ-chains. PBMCs were taken pre- and at week 1 of ibrutinib therapy. Purified surface proteins were treated with EndoH, PNGase or no enzymes and analyzed by immunoblotting. The ratio of expression of the two glycoforms of the µ-chain (mature/immature) is shown for each sample. Filled arrow represents the mature glycoform, open arrow represents the immature glycoform.

Figure 6. Basal phosphorylation of SYK is reduced while pSYK inducibility is increased and correlates with the change in sIgM expression in patients on ibrutinib. PBMCs taken pre- and at week 1 of ibrutinib therapy were stimulated with polyclonal control (Ctrl), anti-IgM F(ab')$_2$ (αIgM) or left untreated (NT) (n=12). (**A**) Representative immunoblots of three cases (346, 632 and 489) showing basal expression of SYK phosphorylated at Tyr525/526 (pSYK Y525/526) and total SYK. GAPDH was used as a loading control. (**B**) Immunoblots of two cases (551 and 409) showing anti-IgM induced expression of SYK phosphorylated at Tyr525/526 (pSYK Y525/526) and total SYK. GAPDH was used as a loading control. (**C**) Inducibility of pSYK was calculated as the ratio between anti-IgM F(ab')$_2$ induced pSYK/SYK and NT pSYK/SYK in each CLL sample. Horizontal lines indicate mean values. The statistical significance of difference was analyzed using the Wilcoxon-signed rank test. **P ≤ 0.01. (**D-E**) Correlation between anti-IgM F(ab')$_2$ pSYK inducibility and (**D**) the expression of sIgM at week 1 of ibrutinib therapy or (**E**) the differential increase of sIgM levels determined by flow cytometry. Linear regression and Spearman correlation are shown. Each symbol identifies one individual patient (refer to **Supplementary Table S1**). Open symbols represent U-CLL, closed symbols represent M-CLL.

Figure 1

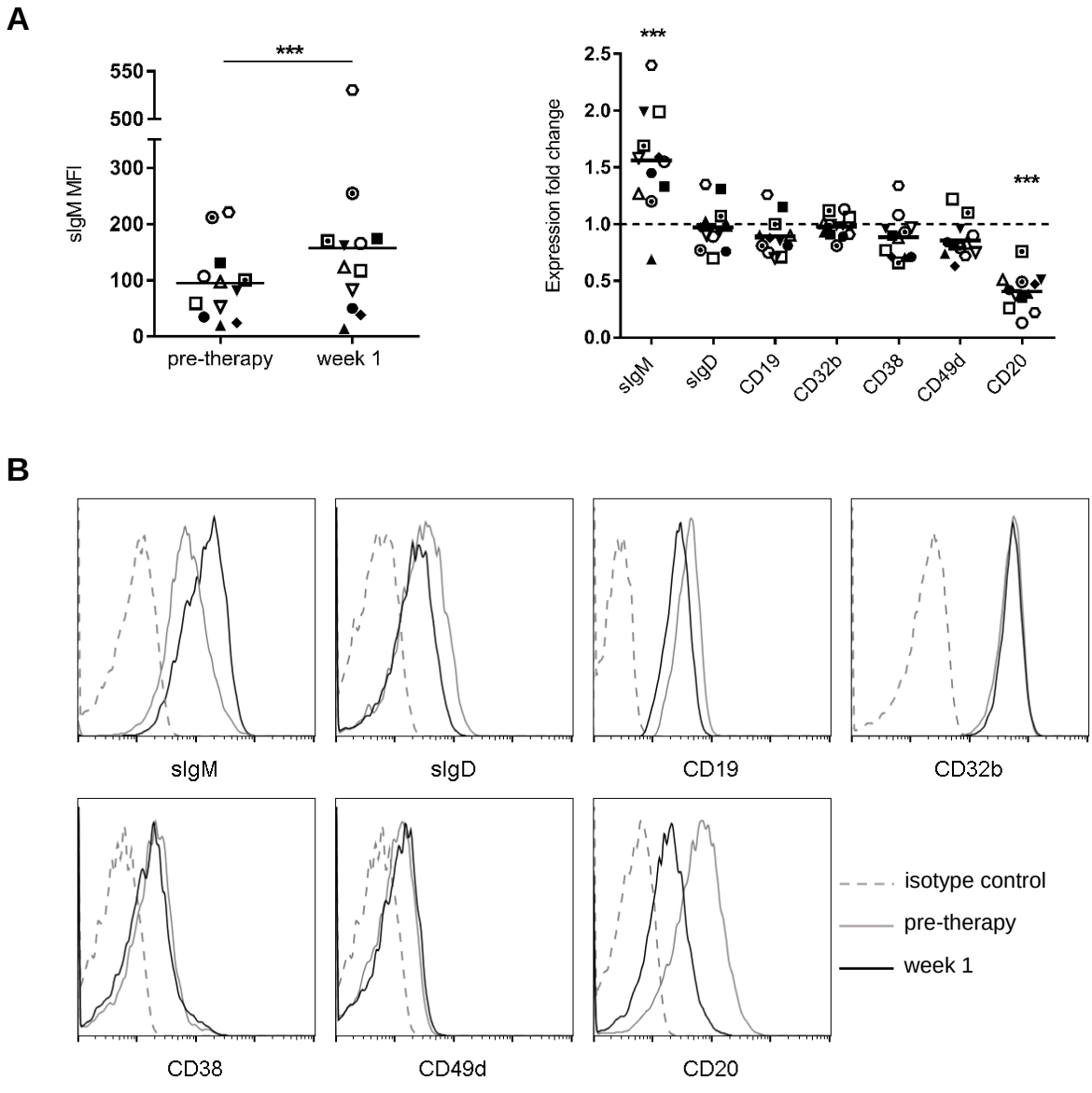
A
***
550
500
300
200
100
0
sIgM MFI
pre-therapy
week 1
***
2.5
2.0
1.5
1.0
0.5
0.0
Expression fold change
***
sIgM
sIgD
CD19
CD32b
CD38
CD49d
CD20
B
sIgM
sIgD
CD19
CD32b
CD38
CD49d
CD20
isotype control
pre-therapy
week 1

Figure 2

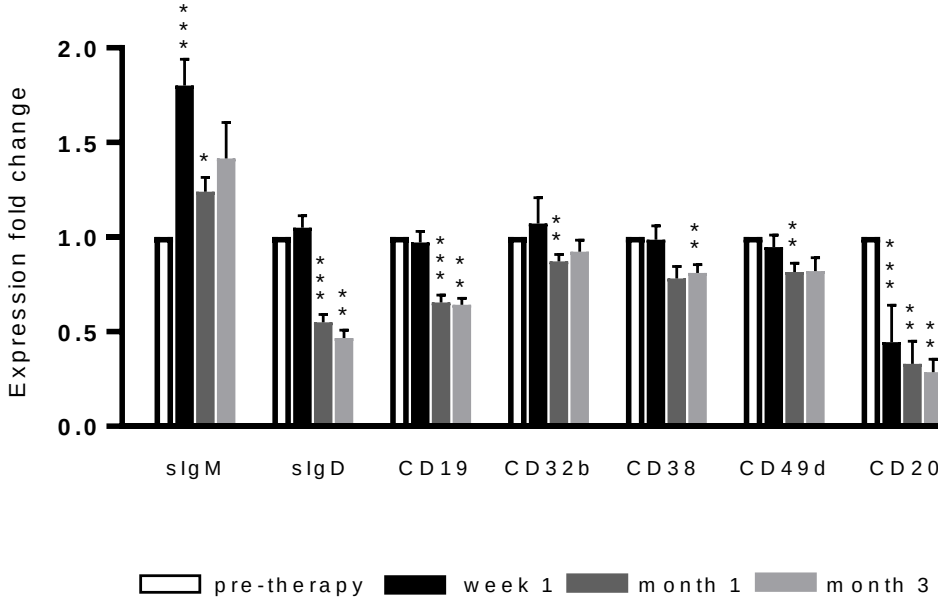
Expression fold change
2.0
1.5
1.0
0.5
0.0
sIgM
sIgD
CD19
CD32b
CD38
CD49d
CD20
pre-therapy
week 1
month 1
month 3

Figure 3

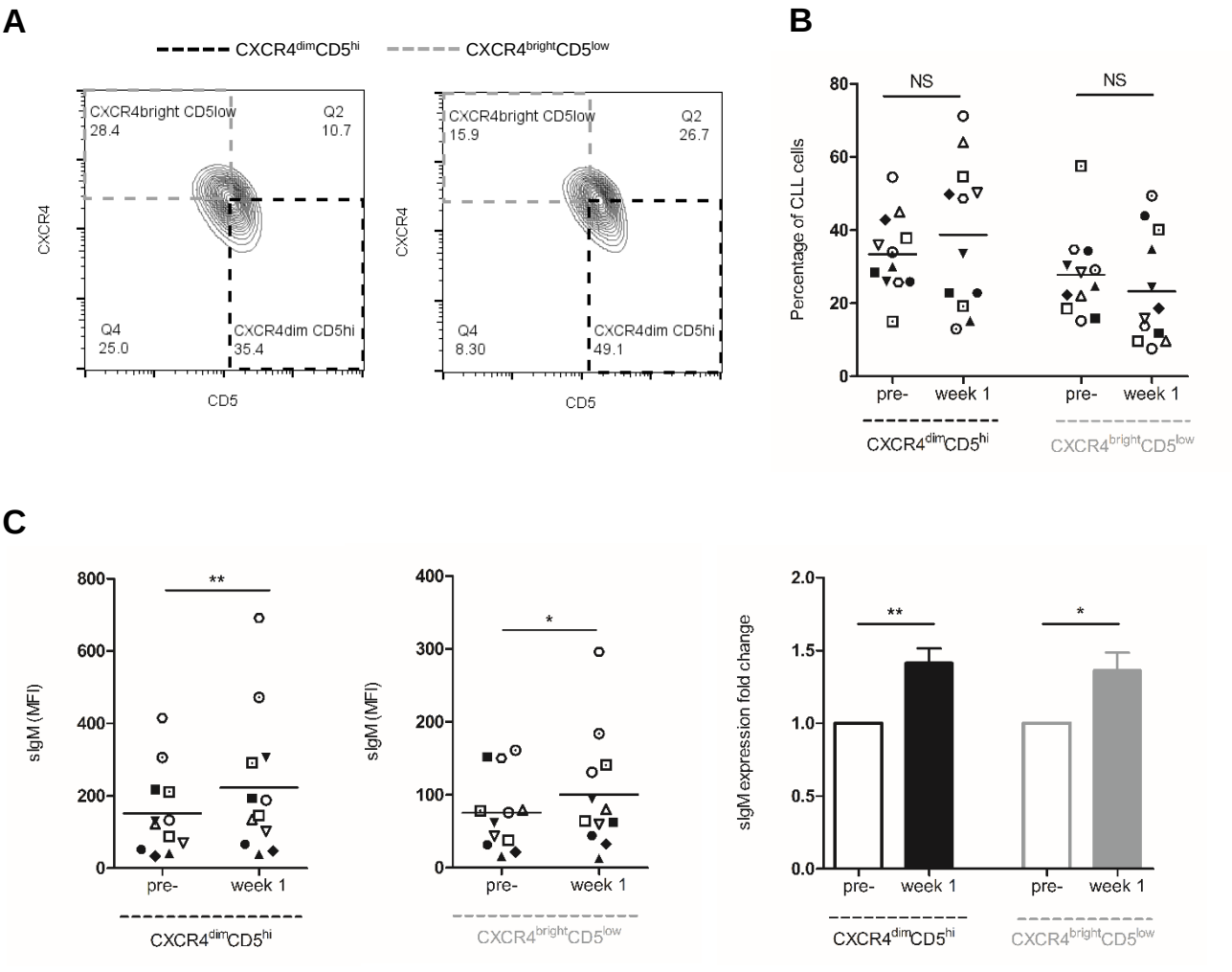
A
CXCR4dimCD5hi
CXCR4brightCD5low
CXCR4bright CD5low
28.4
Q2
10.7
Q4
25.0
CXCR4dim CD5hi
35.4
CXCR4
CD5
CXCR4bright CD5low
15.9
Q2
26.7
Q4
8.30
CXCR4dim CD5hi
49.1
CXCR4
CD5
B
Percentage of CLL cells
NS
NS
pre-
week 1
pre-
week 1
CXCR4dimCD5hi
CXCR4brightCD5low
C
sIgM (MFI)
**
pre-
week 1
CXCR4dimCD5hi
sIgM (MFI)
*
pre-
week 1
CXCR4brightCD5low
sIgM expression fold change
**
*
pre-
week 1
pre-
week 1
CXCR4dimCD5hi
CXCR4brightCD5low

Figure 4

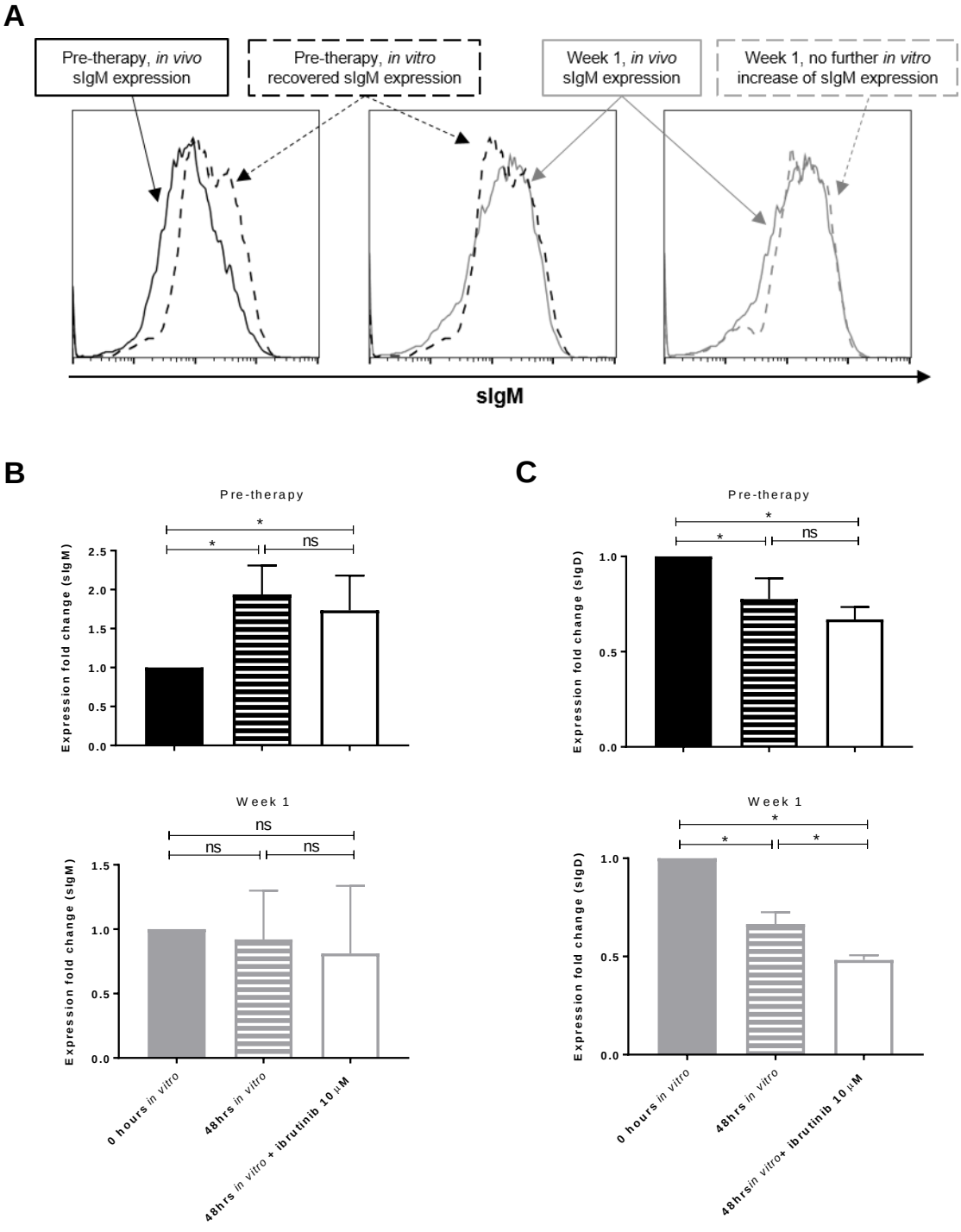
A
Pre-therapy, in vivo sIgM expression
Pre-therapy, in vitro recovered sIgM expression
Week 1, in vivo sIgM expression
Week 1, no further in vitro increase of sIgM expression
sIgM
B
Pre-therapy
Expression fold change (sIgM)
2.5
2.0
1.5
1.0
0.5
0.0
*
*
ns
Week 1
ns
ns
ns
1.5
1.0
0.5
0.0
0 hours in vitro
48hrs in vitro
48hrs in vitro + ibrutinib 10 μM
C
Pre-therapy
Expression fold change (sIgD)
1.0
0.5
0.0
*
*
ns
Week 1
*
*
*
1.0
0.5
0.0
0 hours in vitro
48hrs in vitro
48hrs in vitro+ ibrutinib 10 μM

Figure 5

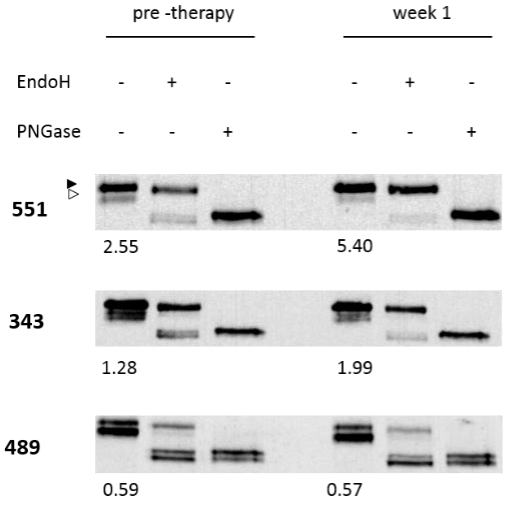

IgM expression (MFI)

Pre	Week 1
221.2	530.3

Pre	Week 1
211.6	254.6

Pre	Week 1
20.2	14.0

Figure 6

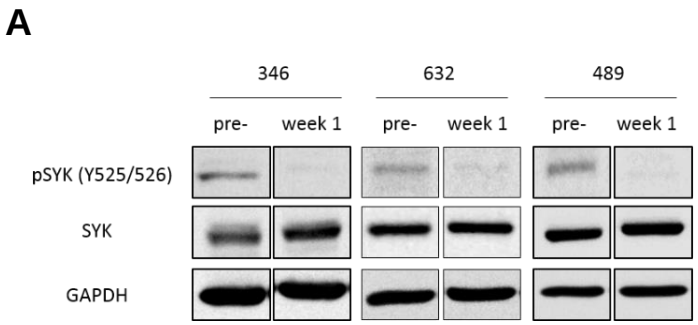
A
346
632
489
pre-
week 1
pre-
week 1
pre-
week 1
pSYK (Y525/526)
SYK
GAPDH

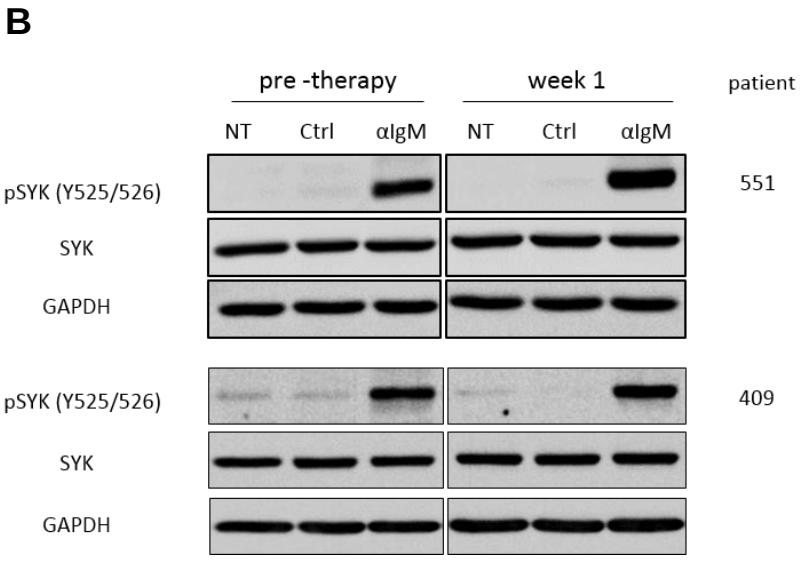
B
pre -therapy
week 1
patient
NT
Ctrl
αIgM
NT
Ctrl
αIgM
pSYK (Y525/526)
SYK
GAPDH
551
pSYK (Y525/526)
SYK
GAPDH
409

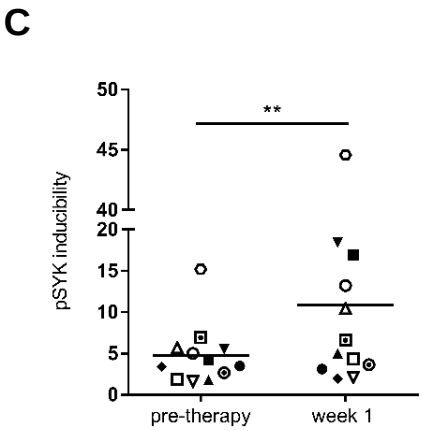
C
**
pSYK inducibility
50
45
40
20
15
10
5
0
pre-therapy
week 1

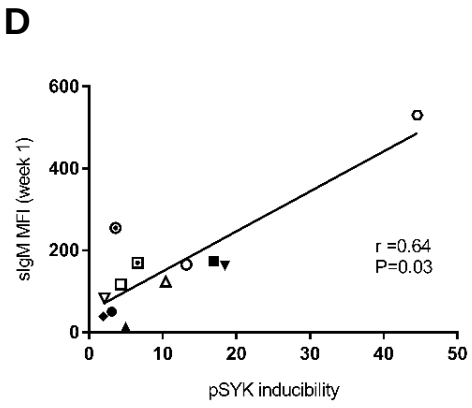
D
sIgM MFI (week 1)
600
400
200
0
r =0.64
P=0.03
0
10
20
30
40
50
pSYK inducibility

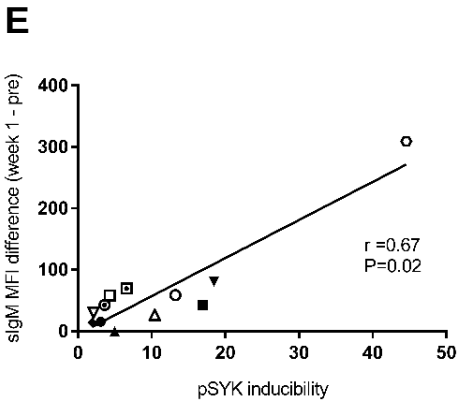
E
sIgM MFI difference (week 1 - pre)
400
300
200
100
0
r =0.67
P=0.02
0
10
20
30
40
50
pSYK inducibility